Non-Line-of-Sight Identification and Mitigation Using Received Signal Strength

Zhuoling Xiao, Hongkai Wen, Andrew Markham,
Niki Trigoni, Phil Blunsom, and Jeff Frolik, *Senior Member, IEEE*

***Abstract*—Indoor wireless systems often operate under non-line-of-sight (NLOS) conditions that can cause ranging errors for location-based applications. As such, these applications could benefit greatly from NLOS identification and mitigation techniques. These techniques have been primarily investigated for ultra-wide band (UWB) systems, but little attention has been paid to WiFi systems, which are far more prevalent in practice. In this study, we address the NLOS identification and mitigation problems using multiple received signal strength (RSS) measurements from WiFi signals. Key to our approach is exploiting several statistical features of the RSS time series, which are shown to be particularly effective. We develop and compare two algorithms based on machine learning and a third based on hypothesis testing to separate LOS/NLOS measurements. Extensive experiments in various indoor environments show that our techniques can distinguish between LOS/NLOS conditions with an accuracy of around 95%. Furthermore, the presented techniques improve distance estimation accuracy by 60% as compared to state-of-the-art NLOS mitigation techniques. Finally, improvements in distance estimation accuracy of 50% are achieved even without environment-specific training data, demonstrating the practicality of our approach to real world implementations.**

***Index Terms*—NLOS identification and mitigation, machine learning, hypothesis testing, localization.**

I. Introduction

In LIGHT of numerous emerging location-aware wireless applications like cooperative communications [1] and mobile queries [2], various localization approaches based on WiFi [3]–[5], UWB [6]–[8], ultrasound [9], etc. have been proposed. UWB and ultrasound-based techniques can provide high localization accuracy but require expensive and specialized infrastructure. In comparison, WiFi-based approaches are a better choice in terms of the cost because they make use of existing WiFi infrastructure including access points, mobile phones, laptops, etc. Therefore, WiFi-based approaches are regarded as the most convenient localization method in indoor environments. Example applications include finding victims in emergencies [10], equipment tracking in hospitals [11], and location-based commerce [12].

However, the accuracy of present WiFi-based localization approaches is not satisfactory especially those based on received signal strength (RSS) because it is detrimentally affected by multi-path effects including reflection, refraction, and diffraction, especially in non-line-of-sight (NLOS) conditions when the received signal contains no direct line-of-sight (LOS) component. Although many indoor localization approaches and indoor propagation models have been proposed to analyze or mitigate the influence of multi-path effects [13]–[15], the mere analysis of multi-path effects without considering the LOS/NLOS conditions is insufficient.

To reduce the negative influence of multi-path effects, NLOS conditions need to be first identified and then be mitigated. The use of LOS/NLOS information can greatly improve the performance of the localization of people and objects inside buildings or in urban landscapes. In general, for the same distance, the RSS in LOS conditions can be over a hundred times stronger than the RSS in NLOS conditions (as shown in Section II), which can result in very large distance estimation errors when employing simple propagation models. Furthermore, since multi-path can impact both LOS and NLOS conditions, accurate path loss models are difficult to ascertain in practice even if NLOS conditions are identified. Therefore, other approaches beyond simple propagation models, e.g., regression, should be employed to estimate distance.

NLOS identification and mitigation techniques developed to date have been primarily investigated for ultra-wide band (UWB) signals [16]–[22]. Due to the large bandwidth of UWB signals, the LOS component can be readily identified and extracted from the received signal. The commonly used techniques in NLOS identification of UWB signals are hypothesis testing [19], [23] and machine learning [22], [24] based on features from the received UWB signals. Features including range estimates [23] (range and error distribution), channel statistics [16]–[19] (RMS delay spread, mean/excess delay, amplitude), and position estimate [20] (ray tracing with map data) of LOS components differ greatly from those of NLOS components. However, with much narrower bandwidths, typical mobile WiFi devices can only report RSS data rather than these detailed features. As such, our goal in this work is to determine whether we can both identify and mitigate LOS/NLOS conditions with this single, rather poor measurement.

NLOS mitigation was achieved in [16], [25], [26] by minimizing the weighted residual of estimated distances. Chen [25] minimized the distance estimation residual by selecting

Manuscript received October 22, 2013; revised March 4, 2014, July 10, 2014, and September 23, 2014; accepted November 10, 2014. Date of publication November 20, 2014; date of current version March 6, 2015. This work was supported by the EPSRC under Grant EP/L00416X/1. The associate editor coordinating the review of this paper and approving it for publication was J. Wallace.

Z. Xiao, H. Wen, A. Markham, N. Trigoni, and P. Blunsom are with the Department of Computer Science, University of Oxford, Oxford OX1 3QD, U.K. (e-mail: zhuoling.xiao@cs.ox.ac.uk; hongkai.wen@cs.ox.ac.uk; andrew.markham@cs.ox.ac.uk; niki.trigoni@cs.ox.ac.uk; phil.blunsom@cs.ox.ac.uk).

J. Frolik is with the School of Engineering, University of Vermont, Burlington, VT 05405 USA (e-mail: jfrolik@uvm.edu).

Color versions of one or more of the figures in this paper are available online at http://ieeexplore.ieee.org.

Digital Object Identifier 10.1109/TWC.2014.2372341

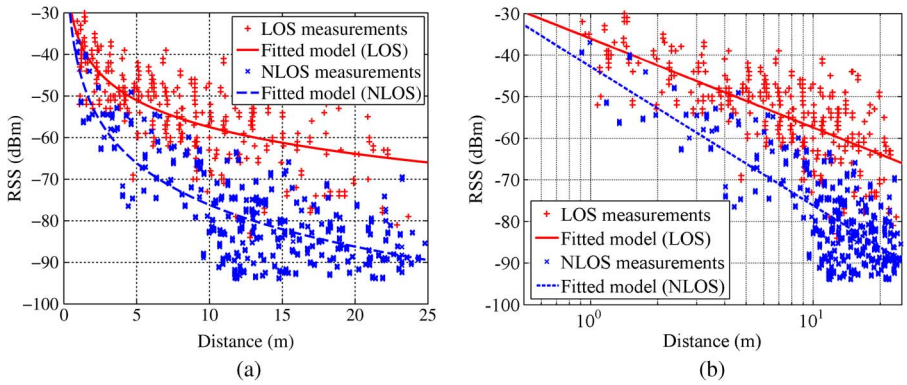

Fig. 1. A large number of RSS measurements were collected in a variety of settings (different access points, distances and environments) in both LOS and NLOS conditions. The propagation model was derived using least square approximations. (a) Linear. (b) Log-distance.

a best subset from available access points (AP). Authors in [16], [26] improved this algorithm to reduce the computation complexity and speed the convergence by using only three distance measurements instead of all available distance measurements. However, these techniques are not suitable for environments with few LOS APs and many NLOS APs. A recent generic NLOS mitigation technique [27] applicable to all wireless systems, tries to reduce the distance estimation errors in NLOS conditions using convex programming. But this approach requires the availability of at least 50% LOS samples, which is also often unrealistic.

In this paper, we propose and compare three NLOS identification and mitigation techniques based only on temporal RSS measurements from WiFi signals. Through observation of a series of temporal RSS measurements from the same location, we explore several features of the RSS data and employ two machine learning algorithms and a Neyman-Pearson testing approach to identify LOS/NLOS conditions and mitigate their impact on distance estimations. The main contributions of this paper are as follows:

- We present methods of NLOS identification and mitigation leveraging only RSS measurements, which greatly improves the potential for RSS-based localization.
- We explore several features from collected RSS measurements, which are shown to be effective in LOS/NLOS discrimination.
- We employ two classifiers based on machine learning and one other based on hypothesis testing to identify the NLOS conditions. These classifiers are shown to perform well even for environments different from which they were trained.
- We use two regressors based on machine learning and one other which fuses hypothesis testing with propagation models to accurately estimate the transmitter-receiver distances in NLOS conditions.
- We present the results of several empirical studies in different environments to show the effectiveness of the proposed techniques in localization in comparison to the existing methods.

The remainder of the paper is organized as follows. Section II formulates the problem and introduces proposed approaches. Section III presents the feature extraction schemes. Section IV proposes three algorithms to identify the NLOS conditions. Section V develops strategies to mitigate the effect of the NLOS conditions. Section VI evaluates the proposed algorithms in various settings. Section VII describes the impacts of our algorithms on positioning system. Section VIII summarizes the paper and discusses future directions.

II. Problem Formulation and Proposed Framework

Problem Formulation: In indoor environments, there are usually many WiFi access points (AP) which are continuously transmitting packets including beacons and user data that can be received with mobile wireless devices. The received signal strength (RSS) of these packets not only determines link quality (LQ) but can also be explored for localization of mobile devices. However, in indoor environments it is very common for the direct path between the transmitter (e.g., AP) and receiver (e.g., mobile devices) to be obstructed by objects such as walls and doors, due to which the receiver is unable to directly 'see' the transmitter. We define this as the non-line-of-sight (NLOS) condition. On the contrary, if the receiver can directly 'see' the transmitter, we have line-of-sight (LOS) conditions.

In multi-path environments it is possible to measure the same RSS for different distances, obstacle, geometries and transmission powers, as shown in Fig. 1. Although a single RSS sample tells us little about the transmitter-receiver distance and LOS/NLOS conditions, a set of T $(T \gg 1)$ temporal RSS samples from a certain receiver position L, denoted by $\langle P^{(1)}, \cdots, P^{(T)} \rangle$, can provide us with much more information. Given these RSS measurements, we aim to infer whether the transmitter and the receiver are in LOS or NLOS conditions $(b = 1/-1)$, called NLOS **identification**, and estimate the transmitter-receiver distance (d), called NLOS **mitigation**.

Proposed Framework: The proposed framework has two major stages: training and testing, as shown in Fig. 2. The training stage consists of the following four steps. 1) An extensive indoor measurement campaign is performed to collect training data, including RSS, and receiver locations which are later used to derive the transmitter-receiver distances and LOS/NLOS conditions with the aid of the floor plan. Suppose we have obtained temporal RSS samples $\langle P_k^{(1)}, \cdots, P_k^{(T)} \rangle$, LOS/NLOS conditions b_k, and transmitter-receiver distance d_k

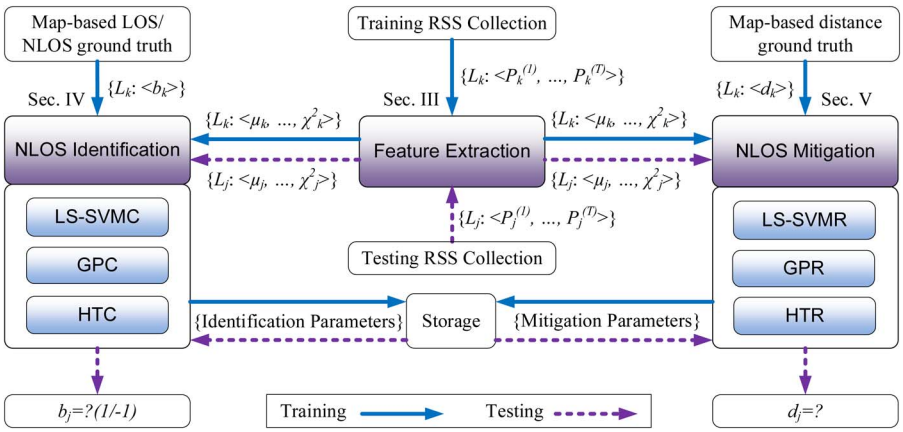

Fig. 2. The system architecture of the proposed NLOS identification and mitigation system.

from N locations $L_k(k = 1, \cdots, N)$ which can be used to train the identification and mitigation models. 2) Then a set of M features including the mean, χ^2 goodness of fit, etc., denoted with $\langle x_k^{(1)}, \cdots, x_k^{(M)} \rangle$ are extracted from the training RSS which are identified to be effective in distinguishing LOS and NLOS conditions and estimating transmitter-receiver distances even in NLOS conditions. 3) Then the parameters of NLOS identification/mitigation algorithms are learned and stored from these features, together with the LOS/NLOS conditions ground truth, and transmitter-receiver distances with the aid of the floor plan. Note that the parameters learned from training are different for each algorithm proposed and are specified in detail in Sections IV and V.

The testing stage has three steps. 1) A new set of RSS data, denoted with $\langle P_j^{(1)}, \cdots, P_j^{(T)} \rangle$, are collected in a new location L_j. 2) The same set of features $\langle x_j^{(1)}, \cdots, x_j^{(M)} \rangle$ are extracted from the RSS set $\langle P_j^{(1)}, \cdots, P_j^{(T)} \rangle$. 3) Then with identification/mitigation parameters from training stage, the proposed NLOS identification/mitigation algorithms predict the LOS/NLOS conditions $(b_j = 1/-1)$ and the transmitter-receiver distance (d_j). Note that the LOS/NLOS condition from NLOS identification is only explicitly used in HTR, but not in LS-SVMR and GPR, as discussed in detail in Section V.

In this study we propose and compare three distinct NLOS identification algorithms based on machine learning techniques and hypothesis testing, namely least square support vector machine classifier (LS-SVMC), Gaussian processes classifier (GPC), and hypothesis testing classifier (HTC). LS-SVMC has a low computational cost compared with other machine learning techniques while GPC has slightly higher identification accuracy. We also present three algorithms to perform NLOS mitigation including least square support vector machine regressor (LS-SVMR), Gaussian processes regressor (GPR), and hypothesis testing regressor (HTR). LS-SVMR and GPR can explicitly predict the transmitter-receiver distances even in NLOS conditions. However, the hypothesis testing algorithm cannot predict distances directly; it first uses the Hypothesis Testing Classifier (HTC) to infer LOS/NLOS conditions, and then selects the appropriate radio propagation model for distance estimation depending on the LOS/NLOS outcome.

III. Feature Extraction

In this section, through observation of multiple RSS samples in LOS and NLOS conditions, we identify several key features from the collected RSS measurements useful for identifying NLOS conditions, including the mean, standard deviation, kurtosis, skewness, Rician K factor, and χ^2 goodness of fit, etc. Each feature is derived from a set of T (e.g., $T = 10$–20) RSS samples $[P^1, \cdots, P^{(T)}]$ collected at a particular location over a short period of time (e.g., 1 s) from one AP. All NLOS identification and mitigation algorithms in this study are developed based on these features.

Mean and Standard Deviation (μ, σ_s) from RSS data can help NLOS identification with features below.

Kurtosis $(\mathcal{K})$ measures the peakedness of the probability distribution. Generally, RSS measurements in LOS conditions are more centralized than samples in NLOS conditions because the dominant LOS signal is much stronger in terms of energy.

Skewness $(\mathcal{S})$ measures the asymmetry of the probability distribution. The skewness of Rayleigh distribution is a constant (approx. 0.63) which is generally larger than the skewness of Rician distribution. In other words, the LOS measurements should have lower skewness than the NLOS measurements.

Rician K Factor (K_r) is defined as the ratio between the power in the direct path and the power in other scattered paths $K = \nu^2/(2\sigma^2)$ [28]. Existing theoretical and empirical studies have shown that there is a link between the Rician K factor and the presence of LOS conditions [29]. Specifically, in NLOS conditions where no direct path exists, the Rician K factor is expected to be close to zero.

χ^2 Goodness of Fit (χ^2) measures the distance between RSS measurements and the underlying Rician distribution. Compared with other scattered signals, the LOS signal reacts minimally to the environments, which leads to different empirical distributions and thus different χ^2 in LOS and NLOS conditions.

The log-mean $(\hat{d})$ is designed primarily for NLOS mitigation. We convert the RSS to logarithmic space because there is a linear relationship between the logarithmic distance and RSS.

Feature Distributions are also derived for hypothesis testing from theory and empirical data. Our data indicates that $\mathcal{K}$ follows closely log-normal distribution, the same as the Kurtosis

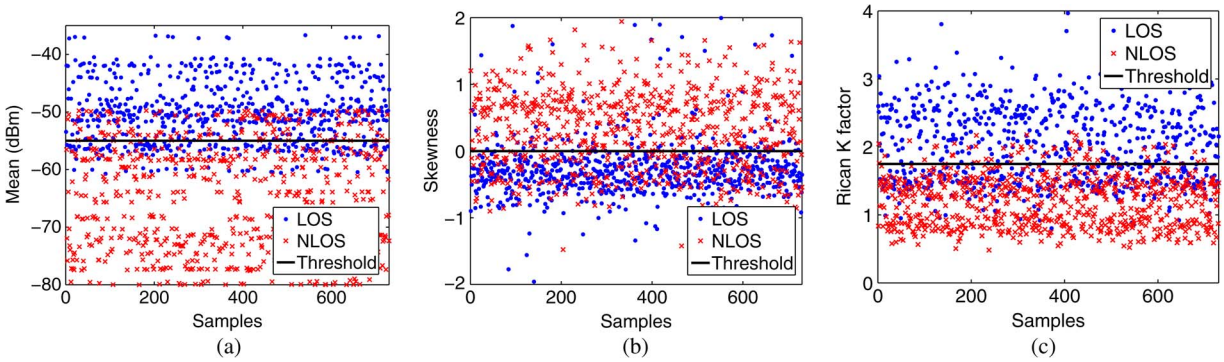

Fig. 3. Illustration of how different features can distinguish between LOS and NLOS conditions. (a) Mean (misclassification 26.46%); (b) Skewness (misclassification 29.92%); (c) Rician K factor (misclassification 28.79%).

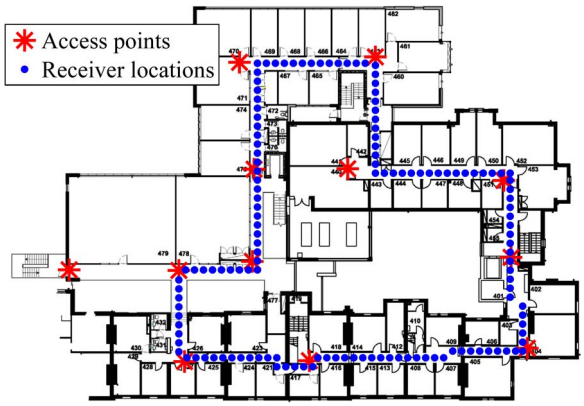

Fig. 4. Map of the office site (65 m × 45 m). Access points and receiver locations are marked.

of UWB signals [16]. In addition, we also find μ, $\mathcal{S}$, K_r, and χ^2 follow closely the Gaussian distribution. Our preliminary experiments show that σ_s does not improve hypothesis testing accuracy and hence we do not discuss its distribution. Fig. 3 illustrates the values of some typical features in different locations under both LOS and NLOS conditions. It is observed that the mean (Fig. 3(a)), the skewness (Fig. 3(b)), and the Rician K factor (Fig. 3(c)) each can individually achieve an identification accuracy of around 70 percent alone with a single threshold estimated using least squares. By fusing features, we can achieve an identification accuracy of around 95 percent with techniques discussed below.

IV. NLOS Identification

The training data for the NLOS identification and mitigation including the RSS, NLOS conditions, and distances were collected in the corridors of our experimental site shown in Fig. 4. We recorded the RSS from all access points marked in Fig. 4 at locations distributed every 1 meter in the corridors. At each location, the LOS/NLOS condition and the distance to each access point were later derived from the recorded locations with the aid of the map. Details of the experiment setup and how we collected data can be found in Section VI. Based on the set of features extracted from the RSS, the task here is to decide whether a given set of RSS samples corresponds to LOS or NLOS conditions.

A. Least Square Support Vector Machine Classifier (LS-SVMC)

Recall that our algorithm is designed for use in mobile devices. As such, the quality of generalization and ease of training are the two highest priorities in the selection of machine learning algorithms. Therefore, we propose using the Support Vector Machine (SVM), a supervised machine learning algorithm that can be used as a classifier to separate data sets with different features and whose capabilities in these two aspects is generally better than other machine learning approaches [30].

Given a set of N training items $\{x_k, b_k\}_{k=1}^N$ where x_k is the kth input consisting of a subset of features described in Section III and $b_k \in \{-1, 1\}$ indicates LOS/NLOS conditions ($b_k = 1$ LOS and $b_k = -1$ NLOS), linear machine learning algorithms are designed to separate the data set in the following form.

$$b(x) = \text{sign}\left[w^T \varphi(x) + w_0\right] \tag{1}$$

in which sign is the signum function, w and w_0 are weight parameters learned from the training data using optimization (3) discussed below, and $\varphi(\cdot)$ is the predetermined feature mapping function. Since the LOS/NLOS RSS measurements are not linearly separable as shown in Fig. 3, we use a Gaussian radial basis function (RBF) to get a better result than a linear feature mapping [31]:

$$k(x, x_k) = \varphi(x)^T \cdot \varphi(x_k) = \exp\left[-\frac{\|x - x_k\|_2^2}{2\sigma^2}\right] \tag{2}$$

where σ^2 is the hyperparameter learned from the training data using (3).

To avoid the quadratic programming problem of SVM, LS-SVM [32] is used in this study, which simplifies the optimization to learn the weights w, w_0, and the penalty of misclassification e as follows.

$$\begin{aligned} \underset{w, w_0, e, \sigma^2}{\arg\min} \quad & \frac{\|w\|^2}{2} + c\frac{1}{2}\sum_{k=1}^N e_k^2 \\ \text{s.t.} \quad & b_k\left[w^T \varphi(x_k) + w_0\right] = 1 - e_k, \ \forall k \end{aligned} \tag{3}$$

where c is the weighting factor that controls the tradeoff between training error and model complexity. It has been proven that the optimization problem in (3) is a linear programming problem [32], which can be solved with its Lagrangian dual and Karush-Kuhn-Tucker (KKT) conditions [33].

After we have ascertained the model parameters w_0, σ^2 from the training data with (3), the prediction of LS-SVMC is given by

$$b(x) = \text{sign}\left[\sum_{k=1}^{N} \lambda_k b_k k(x, x_k) + w_0\right] \tag{4}$$

where λ_k is the Lagrange multiplier, and $k(x, x_k)$ is the kernel function presented in (2).

B. Gaussian Processes Classifier (GPC)

Gaussian processes have gained much interest in recent years [34]. Their explicit formulation makes it possible to both make probabilistic predictions and infer accurate model hyper-parameters, which provides precise trade-off between data fitting and smoothing. In addition, their low computational complexity make Gaussian processes suitable for mobile devices with small data sets [35], such as our application.

To develop classifiers based on Gaussian processes, we implement least-square classification which ignores the discreteness of the target value and treats it as a regression problem. Given the training data $\{x_k, b_k\}_{k=1}^N$, which are the same as for LS-SVMC, the LOS/NLOS conditions for a given data point x is estimated as

$$b(x) = \text{sign}\left[w^T \varphi(x) + n\right] \tag{5}$$

where the weights $w \sim \mathcal{N}(\mathbf{0}, \Sigma_p)$ and the measurement noise $n \sim \mathcal{N}(0, \sigma_n^2)$. Given a training set $\{x_k, d_k\}_{k=1}^N$ where x_k is the kth input consisting of a feature subset described in Section III and d_k is the ground truth distance of the kth sample, rather than search for weights w as in LS-SVMC, we find that:

$$b \sim \mathcal{N}\left(0, k(x, x') + \sigma_n^2 I_n\right) \tag{6}$$

where I_n is the identity matrix and the covariance function or kernel function $k(x, x_k) = \varphi(x)^T \Sigma_p \varphi(x_k)$. Note that it is usually assumed that the mean of the Gaussian processes observation is zero everywhere.

With noisy observations, the joint distribution of the observed target values and the function values under the Gaussian prior can thus be written as

$$\begin{bmatrix} b \\ b^* \end{bmatrix} \sim \mathcal{N}\left(0, \begin{bmatrix} k(x, x^*) + \sigma_n^2 I & k(x, x^*) \\ k(x, x^*) & k(x^*, x^*) \end{bmatrix}\right) \tag{7}$$

where (x, b) is the training set and (x^*, b^*) is the test set. Then the conditional joint posterior distribution on the observation $p(b^*|b)$ is Gaussian with mean and variance:

$$\mathbb{E}[b^*|b] = k(x^*, x)\left(k(x, x) + \sigma_n^2 I\right)^{-1} b \tag{8}$$

and variance

$$\text{cov}[b^*|b] = k(x^*, x^*) - k(x^*, x)\left(k(x, x) + \sigma_n^2 I\right)^{-1} k(x, x^*). \tag{9}$$

Note that the mean prediction is a linear combination of kernel functions, each one centered on a training point, that is

$$\mathbb{E}[b^*|b] = \sum_{i=1}^{n} \alpha_i k(x_j, x^*) \tag{10}$$

where α_i is the ith element of the vector $\left(k(x_j, x^*) + \sigma_n^2 I\right)^{-1} b$ and x_j is a vector representing the jth feature of the training data set.

The kernel function used for this study is as follows:

$$k(x, x^*) = \sigma_0^2 \exp\left(-\frac{|x - x^*|_2^2}{2l}\right) + \sigma_n^2 x^T x^* \tag{11}$$

where the hyper-parameters σ_0 and l are the amplitude and length scale which can be learned from the training data by minimizing the negative log marginal likelihood with respect to the hyper-parameters [36].

The least-square classification is simple and effective, but generally the misclassification rate is slightly higher than other approaches, such as neural networks [37]. Other approximation methods like Laplace approximation [38], [39] can provide more accurate predictions, but these approaches are very computationally expensive and thus not appropriate for mobile devices.

C. Hypothesis Testing Classifier (HTC)

The HTC can identify NLOS conditions with only least square approximation of the means and variances of features. Compared with LS-SVMC and GPC which are accurate but expensive in terms of training cost, HTC skips the expensive training phase at the cost of degraded performance and flexibility.

To identify the LOS/NLOS conditions, we employ the well-known likelihood ratio test where the two competing hypotheses (LOS/NLOS) are defined as

$$\begin{aligned} H_l: &\quad h \le h_t, \text{ LOS conditions } (b = 1), \\ H_n: &\quad h > h_t, \text{ NLOS conditions } (b = -1). \end{aligned} \tag{12}$$

That is, what we need is a proper function h and a threshold h_t to identify the NLOS conditions.

Recall that only the five features μ, $\mathcal{K}$, $\mathcal{S}$, K_r, and χ^2 in Section III help improve the identification accuracy in hypotheses testing. Denote the five features as $x^{(i)}$, $i = 1, \cdots, 5$, and the joint distribution of M $(1 \le M \le 5)$ features with $p(x^{(1)}, \cdots, x^{(M)}|H)$. Since the joint distribution requires the convolution of the PDFs, the computation complexity could be extraordinarily high. To make the algorithm practical, we adopt a suboptimal solution which assumes the variables are independent. Then h is defined as

$$h = \frac{p\left(x^{(1)}, \cdots, x^{(M)}|H_l\right)}{p\left(x^{(1)}, \cdots, x^{(M)}|H_n\right)} = \prod_{i=1}^{M} \frac{p\left(x^{(i)}|H_l\right)}{p\left(x^{(i)}|H_n\right)} \tag{13}$$

where $p(x^{(i)}|H_l)$ and $p(x^{(i)}|H_n)$ are the distributions of feature $x^{(i)}$ in LOS and NLOS conditions, and the threshold $h_t = 1$.

To provide evidence for the validity of the suboptimal solution, we first learn joint distributions $p(\mu, \mathcal{K}, K_r|H_l)$ and $p(\mu, \mathcal{K}, K_r|H_n)$ from 29 700 sets of features extracted from all RSS we collected in the experiments discussed in Section VI. Then we count the cases when the learned joint distributions

without independence assumption and the suboptimal solution make opposite decisions, e.g., $\prod_{i=1}^{M} \frac{p(x^{(i)}|H_l)}{p(x^{(i)}|H_n)} < 1$ when $\frac{p(x^{(1)},\cdots,x^{(M)}|H_l)}{p(x^{(1)},\cdots,x^{(M)}|H_n)} > 1$ or the other way around. We observed only 2.02% of such events, which justifies the use of the suboptimal solution, especially in light of its significantly reduced computation requirements.

V. NLOS Mitigation

In this section, we present three algorithms, including LS-SVMR, GPR, and HTR, to accurately estimate the transmitter-receiver **distances** in LOS and NLOS conditions. In addition, we also make comparisons between the cost and performance of these algorithms in the context of our application.

A. Least Square Support Vector Machine Regressor (LS-SVMR)

The training data of the LS-SVMR are various subsets of features extracted from the RSS samples (input) and the estimated transmitter-receiver distances (output), denoted with $\{x_k, d_k\}_{k=1}^{N}$. The regressor is very similar to the classifier on the optimization problem. The regressor is a function from $\mathbb{R}^n$ to $\mathbb{R}$.

$$d(x) = w^T \varphi(x) + w_0 \tag{14}$$

where $d(x)$ is the estimated distance with input x using LS-SVMR.

The distances between the support vectors and the separating hyperplane are maximized by (15).

$$\begin{aligned} \underset{w,w_0,e}{\arg\min} \quad & \frac{\|w\|^2}{2} + c\frac{1}{2}\sum_{k=1}^{N} e_k^2 \\ \text{s.t.} \quad & d_k = w^T \varphi(x_k) + w_0 + e_k, \ \forall k. \end{aligned} \tag{15}$$

where c is also the weighted factor as in (3) and e_k is the regression penalty learned from the optimization problem (15). Similar to the classification optimization problem (3), the regression problem (15) can also be solved by standard optimization tools.

B. Gaussian Process Regressor (GPR)

As we use least-square classification in GPC, the regression for Gaussian processes is almost identical to the classification in Section IV-B with a single difference in the training and testing output. The output in the classification is the LOS/NLOS labels while for regression it is the transmitter-receiver distance. Therefore, given the same training data as in LS-SVMR for Gaussian processes regression $\{x_k, d_k\}_{k=1}^{N}$, the linear regression model with Gaussian noise for regression is

$$d(x) = w^T \varphi(x) + n \tag{16}$$

where $w \sim \mathcal{N}(\mathbf{0}, \Sigma_p)$ and the measurement noise $n \sim \mathcal{N}(0, \sigma_n^2)$. The rest of the regression is identical to the process from (6)to (11) in GPC with continuous distance d in place of discrete labels b.

Compared to LS-SVMR, the training phase of GPR is more expensive because it takes all training and testing samples which might be thousands of samples as a joint Gaussian distribution and predicts the output as a conditional mean rather than only maximizing the distances between the supporting vectors and the separating hyperplane in LS-SVMR.

C. Hypothesis Testing Regressor

In general, NLOS mitigation is achieved by regression. However, since hypothesis testing yields binary decision, we use different propagation models based on the decision. Many propagation models have been developed so far. For instance, the log-normal propagation model:

$$P(d)[\text{dBm}] = P(d_0) + 10\gamma \log \frac{d}{d_0} + WAF + X_\sigma \tag{17}$$

in which $P(d)$ is the path loss in a location d meters away from the AP, d_0 is the reference distance, γ is the distance power loss coefficient, WAF is the wall attenuation factor which accounts for both real walls in the environment and other minor obstacles like the cases of the mobile devices or access points, and X_σ is a zero-mean Gaussian distributed random variable with variance σ^2 to account for shadowing.

NLOS mitigation is achieved by incorporating HTC and such propagation models. For LOS and NLOS conditions the parameters in (17) (especially γ and σ) can vary greatly thus producing significant errors in distance estimation should inappropriate parameters be used. Therefore, we first identify the LOS/NLOS conditions using HTC and then estimate the transmitter-receiver distances with different propagation models for LOS and NLOS conditions. Specifically, we use different propagation parameters including γ, σ, and WAF, approximated by least-squares from the training data, for LOS and NLOS conditions. For instance, incorporating the LOS/NLOS conditions into (17) makes HTR as follows.

$$P(d) = \begin{cases} P(d_0) + 10\gamma^L \log \frac{d}{d_0} + WAF^L + X_\sigma, & H = H_l, \\ P(d_0) + 10\gamma^N \log \frac{d}{d_0} + WAF^N + X_\sigma, & H = H_n. \end{cases} \tag{18}$$

The incorporation of LOS/NLOS conditions with other propagation models is similar.

Compared to LS-SVMR and GPR, HTR only requires least-square approximation of the propagation parameters (γ, σ, and WAF) and feature distribution parameters (mean, variance) from training data. However, the reduced training phase and the independence assumption between features will degrade the distance estimation performance.

VI. Evaluation

This section demonstrates and evaluates the proposed algorithms through extensive data collection at different times and places. To make the evaluation reliable, RSS samples are collected during different periods of the day to account for time variability, and in three experimental sites with different floor plans to account for the environment variability.

A. Experiment Setup

Sites: The proposed NLOS identification and mitigation algorithms were evaluated in three different real-world settings, namely an office, a basement, and an attic. The site shown in Fig. 4 is the 4th floor of a multi-storey office building with a stone and brick construction, reinforced with metal rebars. The majority of RSS samples in this site were collected along the corridors surrounded by rooms. The site shown in Fig. 9 is a basement where the RSS samples were collected in both corridors and rooms which are surrounded by soil and rocks. Fig. 10(a) shows the layout of the attic test location. All access points and locations where RSS samples are collected in three experiment sites are marked in Figs. 4, 9, and 10(a).

Devices and Implementations: To make the proposed approaches more readily implementable for localization, different mobile devices, including Acer Aspire One ZG5 running Ubuntu 3.2.0 and Huawei U8160 mobile phones running Android 2.3.3, were utilized in the experiments. To account for the various relative antenna orientations that may occur between transmitters and receivers, the mobile device always kept face up and oriented parallel to the trajectories taken so the relative orientation changed with movement during the data collection. Measurements from over ten different mobile devices were fused in the experiments to account for hardware variations between these mobile devices.

Ground truth: To provide accurate ground truth, numbered labels were placed along corridors and within rooms on a 1 meter grid where experiments were conducted. We recorded the current time and label number manually when the mobile device reached a certain label. The labels are then mapped to locations on the floor plan to obtain the ground truth of LOS/NLOS conditions and transmitter-receiver distances. With the settings of access point locations and data collection locations, the transmitter-receiver distances vary from 0.8 meters to 25 meters with maximum discretization step of 1 m.

Data collection: We implemented two approaches to collect RSS samples: passive and active. With the passive approach, a mobile device scans for beacons transmitted by the various APs and then records RSS values. Given that the default beacon interval is 102.4 ms (or 51.02 ms for some APs), it is possible to collect 10–20 samples from each AP per second. APs can be configured to send beacons as rapidly as 1000 Hz, but this involves reconfiguring infrastructure, which one does not necessarily have access to. In comparison, during the active approach, a mobile device broadcasts probe requests and obtains RSS samples from probe responses. The active approach collects data much more quickly (can be over 1000 Hz) than the passive approach at the cost of higher energy consumption on the mobile device. In practice, one can switch between the passive approach and the active approach according to the motion of the user, found by monitoring the change in the mean per AP RSS. We used the active approach when the RSS changed rapidly and the passive approach otherwise. We collected 50 to 1000 samples at each given location. Since the numbers of LOS and NLOS samples differ in various scenarios, we collect half of the samples in LOS conditions and the other half in NLOS conditions for training and testing.

B. Data Sets and Training

The accuracy of NLOS identification techniques can be easily decreased by interference from people walking around and other signal noise. Although people around may not block the LOS signal, they may block and absorb other components of the received WiFi signal which leads to the variation of the measurement distribution. Moreover, from the long-term perspective of practical use, it is impossible to avoid interference from people.

Therefore, we have two separate categories of RSS samples in the data sets to account for the interference from people. The first group of samples was collected during nights when there were few people walking around to absorb and block the WiFi signal (called *static environment* hereafter). The other group of samples was collected during busy office hours when there were many people walking around the corridors, which interfere with the RSS measurements (called *dynamic environment* hereafter). Each of the two groups contains approximately 1500 sample sets, each of which is composed of 1000 RSS samples (3 360 000 RSS samples in total). We divided each sample set into subsets according to the sample size, as discussed in the next subsection, and extract features from each subset. As noted, half of the sample sets in each group were taken from LOS conditions and the other half from NLOS conditions.

After the database of measurements was built, we tested the accuracy of the proposed algorithms using five-fold cross validation. Specifically, we randomly divide all the RSS measurements collected in the office site into five data sets. Then the algorithms were trained with four datasets and tested with the remaining dataset. The training and testing processes were repeated five times until each data set has been tested. Then we calculate the mean accuracy as the performance metric of the algorithm on the whole database. The performance of the classifiers and regressors are discussed in the next subsection.

C. Testing

In this subsection we discuss the performance of the proposed NLOS identification and mitigation algorithms with both the training data and testing data from the office site in Fig. 4. For a given number of features, e.g., three, we performed cross validation with all $\binom{7}{3}$ combinations of the features introduced in Section III. The feature subset with the lowest misclassification rate and distance estimation errors are presented in Tables I and II. We denote the feature subsets with lowest misclassification rate for machine learning techniques (LS-SVMC and GPC) in static and dynamic environments with S_i^L and $D_i^L (i = 1, \cdots, 5)$, respectively. The feature subsets with lowest misclassification rate for HTC in static and dynamic environments are denoted with S_i^H and $D_i^H (i = 1, \cdots, 4)$, respectively. The feature subsets with lowest distance estimation errors for machine learning techniques are denoted with $S_i^R (i = 1, \cdots, 5)$.

NLOS Identification: The performance of the algorithms are measured in terms of missed detection probability p_m (deciding LOS when the RSS samples are from NLOS conditions), false alarm probability p_f (deciding NLOS when the RSS samples

TABLE I
FEATURES IN DIFFERENT FEATURE SUBSETS

Features	Subsets for LS-SVMC and GPC										Subsets for HTC							
	S_1^L	S_2^L	S_3^L	S_4^L	S_5^L	D_1^L	D_2^L	D_3^L	D_4^L	D_5^L	S_1^H	S_2^H	S_3^H	S_4^H	D_1^H	D_2^H	D_3^H	D_4^H
μ	✓	✓	✓	✓	✓	✓	✓	✓	✓	✓	✓	✓	✓	✓			✓	✓
σ_s				✓	✓			✓										
$\mathcal{K}$					✓				✓	✓			✓	✓		✓	✓	✓
$\mathcal{S}$					✓		✓	✓	✓	✓		✓			✓	✓	✓	✓
K_r		✓	✓	✓	✓				✓	✓			✓	✓				✓
χ^2			✓	✓						✓				✓				

TABLE II
FEATURE SUBSETS FOR LS-SVMR/GPR

Subsets	Features						
	μ	σ_s	$\mathcal{K}$	$\mathcal{S}$	K_r	χ^2	$\hat{d}$
S_1^R	✓						
S_2^R	✓						✓
S_3^R	✓					✓	✓
S_4^R	✓				✓	✓	✓
S_5^R	✓	✓			✓	✓	✓

are from LOS conditions), and overall misclassification probability $p_e = p_m + p_f$.

Fig. 5 shows the misclassification rates of the proposed techniques in static and dynamic environments using varying number of features shown in Table I. We can observe that the misclassification rate of LS-SVMC in the static environment is far better than those in the dynamic environment. The best identification errors for LS-SVMC, GPC, and HTC are 0.0648, 0.0599, and 0.1568 in static environments, and 0.1401, 0.1301, and as high as 0.3744 in dynamic environments. The major reason for the poor performance of HTC is that HTC is equivalent to a linear classifier while the majority of LOS/NLOS conditions are not linearly separable, as shown in Figs. 1 and 3, especially with nonlinear features like χ^2 or in dynamic environments, which explains the poor performance of S_4^H and feature sets in dynamic environments.

From Fig. 5(a) and (b), K_r appears in most feature sets in static environments, which proves K_r to be indicative for NLOS identification in static environment. The reason is straightforward: K_r measures the difference between a Rician distribution (LOS condition) and a Rayleigh distribution (NLOS condition). However in dynamic environments, K_r is no longer an essential feature, which indicates that the interference actually blurs the demarcation line between distributions in LOS and NLOS conditions. Instead, the skewness appears in each data set and thus becomes the most crucial feature.

Fig. 6 compares the misclassification rate of LS-SVMC and GPC using different sample sizes in static and dynamic environments. In both static and dynamic environments, the misclassification rates are the lowest when the sample size is 1000 and the largest when the sample size is 50, which indicates that the number of samples collected at each location also impacts the identification accuracy. The reason for the impact of sample size is that a larger number of samples can reduce the influence of noisy RSS samples, which leads to a more precise fit of the samples to a distribution and thus a more accurate result.

The number of packets exchanged during the reception of a standard text email is on average around 30, including the overhead packets like beacons, handshake, and handoff. Based on the above experiments the number of RSS samples from these packets would be sufficient for the proposed technique to provide an acceptable NLOS identification accuracy. An email with picture attachments contains hundreds of MAC layer packets which can make the identification very accurate without any change to the existing protocol stacks or infrastructures.

Summary: The identification accuracy of LS-SVMC and GPC can be up to around 95% with training phase while HTC can greatly reduce the training phase at the cost of lowering the NLOS identification accuracy to 85%. For all three identification techniques, sample size has impact on the accuracy.

NLOS Mitigation: In this subsection, we will discuss the accuracy improvement of distance estimation with NLOS mitigation techniques compared with conventional propagation models.

1) *Standard Propagation Model (SPM)*: This is the first strawman algorithm used for comparison. We used all training RSS data including both LOS and NLOS conditions to estimate γ and *WAF* in (17) with least squares. Note that SPM does not differentiate between LOS from NLOS conditions.
2) *Breakpoint Propagation Model (BPM)*: This is the second benchmark algorithm for comparison [40]. This propagation model incorporates the breakpoint phenomenon [41] into the log-distance propagation model, which makes the breakpoint propagation model [40]. The breakpoint distance can be determined by the first Fresnel zone [42] and takes the typical value of 7 m for WiFi signals between APs and mobile devices in this study [43]. Similarly, we also use least squares approximation to derive other BPM parameters such as γ and *WAF*.
3) *Least Square Support Vector Machine Regression (LS-SVMR)*: This is the first proposed algorithm. Instead of estimating the distance with only the mean of RSS measurements in the propagation models, LS-SVMR takes into account more features of the RSS measurements to estimate the distances.
4) *Gaussian Processes Regression (GPR)*: This is the second algorithm proposed. GPR uses the same feature sets as LS-SVMR.
5) *Hypothesis Testing Regression (HTR)*: This is the third proposed algorithm which fuses HTC which identifies LOS/NLOS conditions and SPM/BPM to improve the distances estimation accuracy. The model given in (18) is used in this section for comparison.

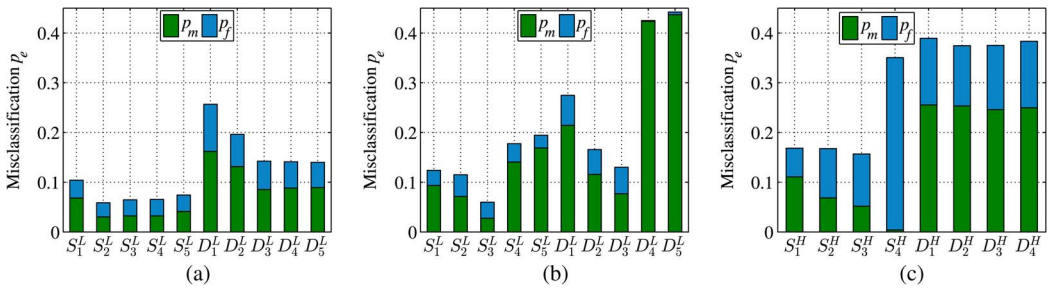

Fig. 5. Missed detection probability (p_m), false alarm probability (p_f), and overall misclassification probability (p_e) of the proposed algorithms, showing the impact of different feature sets. (a) LS-SVMC. (b) GPC. (c) HTC.

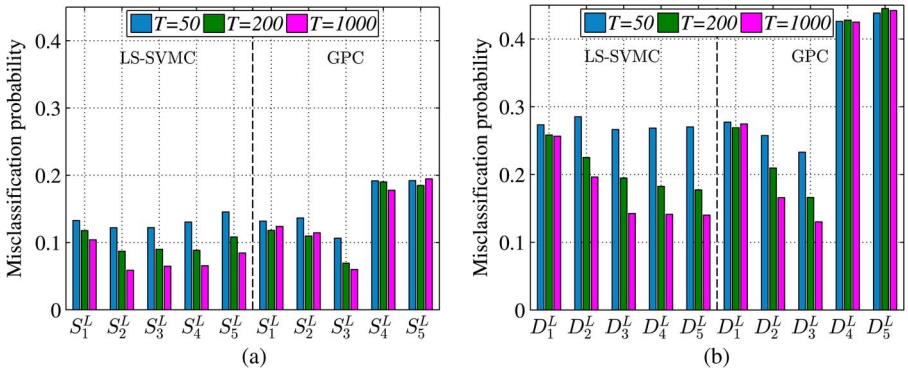

Fig. 6. Overall misclassification probability in (a) static and (b) dynamic environments for different sample size. Features of different sizes are consistent with Table I. (a) Static environments. (b) Dynamic Environments.

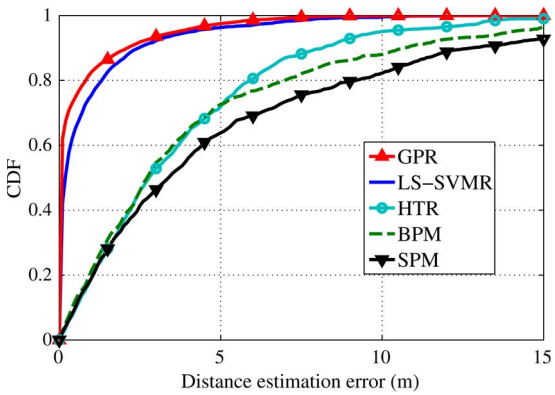

Fig. 7. CDF of various distance estimation methods.

The distance estimation errors of various models are shown in Fig. 7. It is observed that HTR only improves by around 20% compared to BPM. In comparison, both LS-SVMR and GPR greatly outperform other models with the mean error from 6.61 m for SPM to 0.86 m for LS-SVMR and 0.82 m for GPR.

Fig. 8 compares the distance estimation performance of LS-SVMR and GPR with different feature sets. Subsets with different features are shown in Table II. It is observed that the GPR works slightly better than LS-SVMR with the best feature set (S_2^R) while its performance rapidly drops with other feature sets. The impact of limited training on the distance estimation performance is shown in Fig. 8(c). We can observe that the distance estimation accuracy can be improved with more training data. This trend is apparent especially when the percentage of training data is low (less than 40%). Note that there is no overlap between the training and testing data.

It is observed from Figs. 5 and 8 that the identification accuracy and distance estimation errors of LS-SVMC/LS-SVMR are more stable with more noisy features than GPC/GPR. As spline smoothing techniques, both LS-SVM and GP predict a new target by reweighting the vector of training targets to arrive at a weight vector which is then used to form an average over the correlations between the new input point and the training points. The difference between the two methods lies in the reweighting factors for the targets. In our implementation of GPC/GPR, all features share the same length scale to reduce the training computational complexity, which also reduces the feature selection ability of GPC/GPR. Therefore, the performance of GPC/GPR is degraded when noisy features are included. To increase the feature selection ability and make GPC/GPR robust to noisy features, we can implement automatic relevance determination (ARD) in the parameter learning, which, intuitively, learns different length scales for different features.

It is also observed that HTC/HTR always performs worse than LS-SVMC/LS-SVMR and GPC/GPR. The underlying reasons are three-fold. As noted, HTC is equivalent to a linear classifier while the LOS/NLOS conditions are not linearly separable using only RSS. Even more detrimental, the identification errors of HTC still have impact on HTR because HTR is the combination of HTC and propagation models. Moreover, the log-distance propagation model used in HTR is only a rough two-parameter approximation of the actual RSS-distance relation, as shown in Fig. 1. On the contrary, LS-SVMR and GPR can learn a best model in least square sense which can describe the RSS-distance relation much better than a simple log-distance model. Even with only one feature (e.g., the RSS mean), LS-SVMR and GPR perform much better

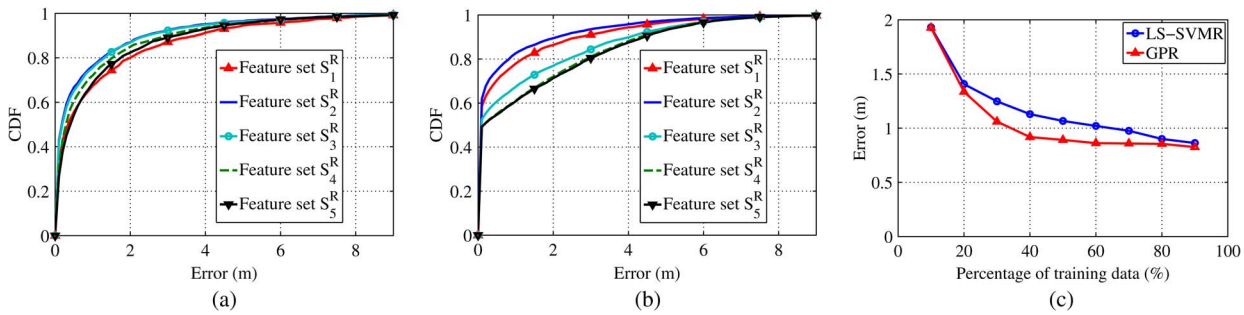

Fig. 8. Comparison of distance estimation performance between LS-SVMR and GPR. (a) LS-SVMR. (b) GPRp. (c) Impact of limited training.

than the HTR—the combination of HTC and the log-distance propagation model. Finally, LS-SVMR and GPR take more useful features into account for distance estimation than the propagation model used in HTR, which further helps improve the distance estimation accuracy.

In addition, Fig. 8 shows that the performance of the regressor does always improve as we add more features. However, only informative features like μ and $\hat{d}$ (please refer to Section III for details) can improve the regression accuracy while noisy features like σ_s could degrade the regression performance. That is why we can observe that the feature set S_2^R that includes both informative features (μ and $\hat{d}$) always performs better than any feature set with more than these two features.

Summary: LS-SVMR and GPR can greatly improve the distance estimation accuracy to around 0.86 m as opposed to over 6.6 m with conventional propagation models. In addition, with a comparatively much shorter training phase, HTR can achieve an accuracy of 3.5 m.

D. Validation

This subsection validates the performance of the proposed algorithms in a different experiment site (basement site) than from where the training data was collected (office site). It is crucial for practical algorithms to work in different sites without per-site training because training is highly labour intensive.

To test the robustness of the two machine learning based NLOS identification and mitigation algorithms over different sites, we use the same set of parameters trained from the static environments in the office site in Fig. 4 to identify and mitigate the NLOS conditions in the basement site as shown in Fig. 9.

The overall misclassification rates of both the LS-SVMC and GPR with the best 3-feature set $S_3^L(\mu, K_r, \chi^2)$ from Fig. 5 are around 0.091 when tested in the basement site, as opposed to 0.065 when tested in the office site. In terms of average distance estimation error, the mean distance estimation error is 2.41 m for LS-SVMR and 2.33 m for GPR in the robustness testing, as opposed to 0.86 m and 0.82 m when they were trained and tested in the office site. The observed errors still far outperform the propagation models by over 60% improvement over SPM.

From the aforementioned experiments, the "general applicability" of the training parameters for machine learning based NLOS identification and mitigation algorithm makes the training phase very easy. Therefore, although the training phase of the machine learning based method is time-consuming and costly, we do not have to train the parameters every time we

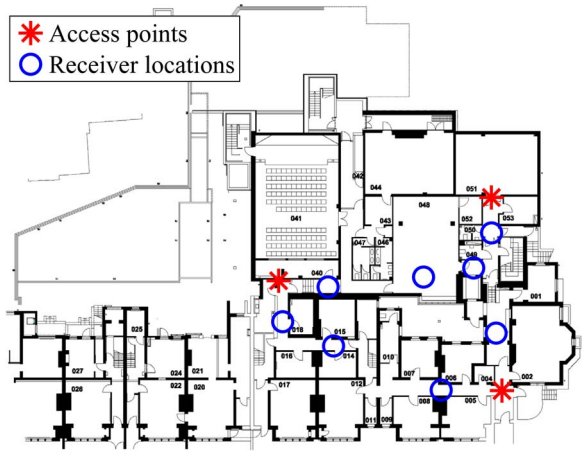

Fig. 9. Map of the basement site (55 m × 40 m). Access points are marked in the maps.

plan to use them. Instead, we could use the same parameters from other applications concerning the NLOS identification and mitigation algorithms. In addition, since RSS is a simple measurement that every WiFi device can provide, potentially we can have a huge amount of crowd-sourced data. Based on such data, it would be possible that an unsupervised learning algorithms such as Expectation Maximization (EM) [44] could help in learning the algorithm parameters.

Summary: In a different environment from where the training parameters are obtained, LS-SVMC and GPC can also obtain over 90% accuracy in NLOS identification. Meanwhile, LS-SVMR and GPR can achieve an accuracy 60% higher than traditional distance estimation approaches.

E. Robustness

It is important that the proposed NLOS identification and mitigation algorithms take into account the impact of different signal properties such as the transmission power level and signal frequency. The goal of the following experiments was to test whether our algorithms are robust against such changes.

Fig. 10(a) shows the experiment scenario of testing the impact of different WiFi signal properties on our NLOS identification algorithms. Four receivers were put inside a room together with eight LOS transmitters which are evenly distributed within the room. Meanwhile, one group of five NLOS transmitters are put in a neighbouring room connected by an open door while the other NLOS group of three transmitters are put outside the

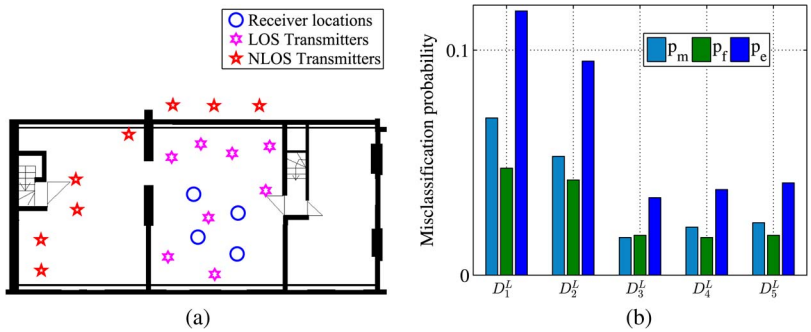

Fig. 10. Experiment site and misclassification rate of LS-SVMC in dynamic environment in testing the robustness of our system against various signal properties. (a) The attic site (17 m × 7 m); (b) The misclassification rates of LS-SVMC.

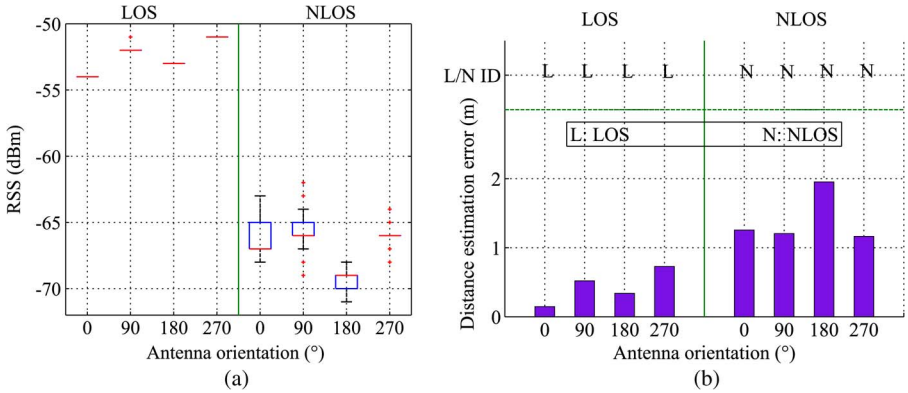

Fig. 11. The impact of antenna orientation on the NLOS identification and mitigation algorithms. (a) The raw RSS. (b) NLOS identification and mitigation accuracy.

room where the transmitters and receivers are separated by a wall built with concrete building materials. Both the LOS and NLOS transmitters are set to work with different transmission power levels ranging from 0 dBm to 20 dBm. In addition, some of the LOS and NLOS transmitters are set to transverse all available WiFi channels (hop to the next legal frequency band periodically) to test the influence of signal frequency on our system.

Transmission Power Level: The misclassification rate for LS-SVMC in this experiment is shown in Fig. 10(b). It is observed that the same feature sets in dynamic environment from Fig. 5 give a misclassification rate as low as 0.0344 for feature set $D_3^L(\mu, \sigma_s, \mathcal{S})$, which further demonstrates the effectiveness of our algorithm. The proposed algorithm performs better in this experiment than in Section VI-C as the extracted RSS features are able to discriminate better the conditions when the transmitter is in the same room as the receiver (LOS) and when the transmitter is in a different room (NLOS).

Signal Frequency: The experiment results show that the switch from one channel to another does not impact our algorithm. The reason is that we are collecting a large number of RSS data, we can "average out" small scale multipath effects which might be more apparent in some channels than others.

Antenna Orientation: We also evaluate the impact of antenna orientations on the proposed algorithms. Fig. 11(a) shows the mean and 75 percentile of the RSS measurements we collected in LOS and NLOS conditions with the same transmitter-receiver distance but different antenna orientations. It is observed that antenna orientations have impact on the RSS, especially in NLOS conditions. However, from Fig. 11(b) we have demonstrated that GPC can identify the LOS/NLOS conditions with 100% accuracy (please see the "L/N ID" at the top of the plot). In addition, GPR can also predict nearly identical distances with different antenna orientations.

Summary: The experimental results show that the proposed NLOS identification and mitigation algorithms are robust against the change of transmission power level, signal frequency, and antenna orientations.

VII. Impact on Positioning System

With the NLOS mitigation techniques in Section VI, we can derive the locations of the mobile devices with trilateration [45]. Then we implemented a particle filter to smooth all the trajectories (200 particles). Fig. 12 compares the trajectories estimated from different localization approaches. All trajectories presented are estimated from the same raw RSS measurements. The trajectories are estimated from (a) ground truth, (b) SPM, (c) Guvenc *et al.* [16], (d) HTR, (e) Fingerprinting (HORUS) [45], (f) BPM, (g) Nawaz *et al.* [27], and (h) LS-SVMR. As the performance of GPR is similar to LS-SVMR, it is not included here.

It is observed from Fig. 12 that the approach proposed by Guvenc *et al.* [16], which selects the AP subset with minimum weighted residual, works fairly well in our experiments.[1] In

[1]Since the mean excess delay and RMS delay spread measurements are not available from WiFi signals, we use the best feature set in our experiments (μ, $\mathcal{K}$, and K_r) instead which are calculated from the directly measurable RSS.

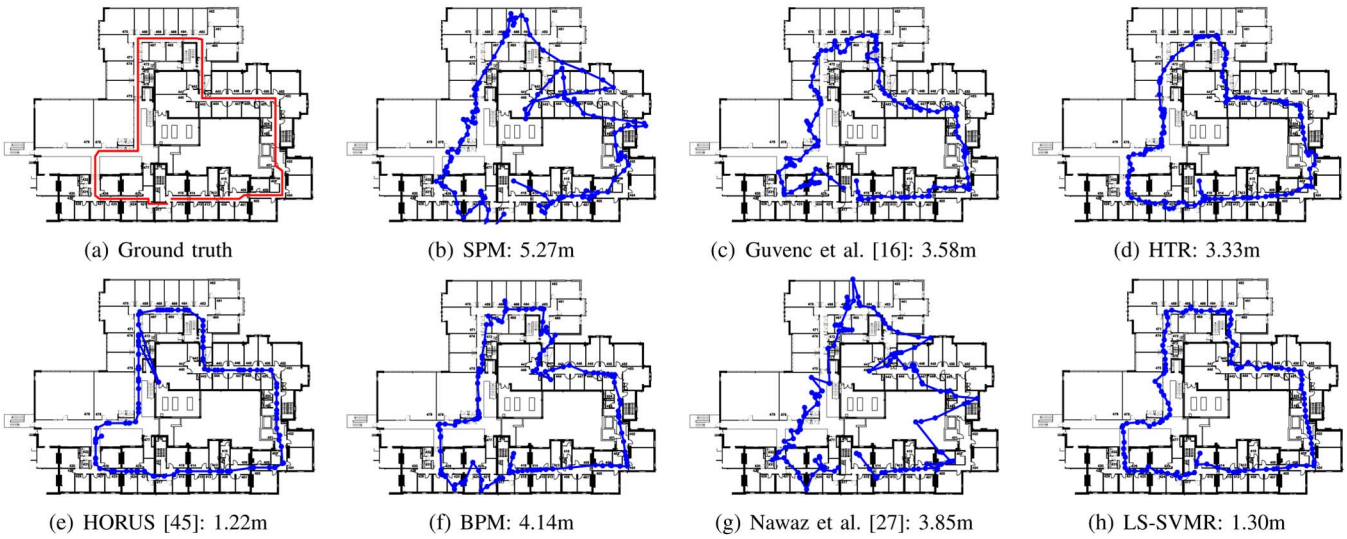

(a) Ground truth (b) SPM: 5.27m (c) Guvenc et al. [16]: 3.58m (d) HTR: 3.33m

(e) HORUS [45]: 1.22m (f) BPM: 4.14m (g) Nawaz et al. [27]: 3.85m (h) LS-SVMR: 1.30m

Fig. 12. Trajectories generated by different algorithms along with the RMS errors: (a) Ground truth, (b) SPM, (c) Guvenc *et al.*, (d) HTR, (e) Fingerprinting (HORUS), (f) BPM, (g) Nawaz *et al.*, and (h) LS-SVMR.

addition, recall that the generic NLOS mitigation approach proposed by Nawaz *et al.* in [27] tries to reduce the estimation errors by assuming that the number of LOS APs is greater than the number of NLOS APs. In our experiments this algorithm results in poor performance at many locations (RMSE up to 10 meters) where NLOS APs outnumber LOS APs.

Fig. 12 also shows that there is only slight improvement in accuracy for the propagation model derived from hypothesis testing results, compared with the generic NLOS identification and mitigation approaches proposed in existing works [16], [27]. The inability of a simple propagation model to capture major features of different complicated indoor environments results in this phenomenon.

We can also see from Fig. 12 that the localization system based on LS-SVMR improves the localization accuracy by 60% compared with the trajectories estimated with the state-of-the-art NLOS mitigation algorithms, which greatly increases the potential of using WiFi-based localization in practical settings.

We also evaluated the positioning experiment settings including AP and receiver locations, attenuation factor distributions in this study with Cramer Rao Lower Bounds (CRLB) [47]. The path loss based theoretical CRLB of the positioning error is 1.31 m, almost the same as the positioning error of the proposed machine learning approaches (approx. 1.30 m), which proves the effectiveness of the proposed methods. The major reasons why the positioning error of the proposed approaches is slightly smaller (less than 1%) than CRLB are a) the assumption of CRLB that each AP has the same distribution for attenuation factor γ but that is not true in practice, especially in indoor environments, and b) the particle filtering which removed outliers and improved the positioning accuracy.

In addition, we implemented the well-known fingerprinting approach HORUS [45] with the same training and testing data as the proposed techniques. It is observed from Fig. 12(e) and (h) that the accuracies of HORUS and LS-SVMR/GPR are comparable. However, one major advantage of the proposed approaches is that LS-SVMR/GPR can be used in different environments (as shown in Section VI-D), which means the proposed techniques do not require per-site training or extra user effort. On the contrary, it is well-known that per-site training is a must for fingerprinting approaches because different sites have different access points and links between the locations and RSS from different access points.

Summary: The proposed NLOS mitigation algorithms can greatly improve the distance estimation accuracy and thus improve the RSS-based localization accuracy by over 60% compared with the state-of-the-art NLOS mitigation algorithms. Performance is also comparable with site-specific fingerprinting approaches.

VIII. Conclusion and Future Work

In this paper, we have proposed three algorithms to address the problem of NLOS identification and mitigation using only WiFi RSS measurements. To our knowledge, this is the first time NLOS identification and mitigation are conducted using only RSS from real experiments with mobile devices. The proposed algorithms can not only accurately identify NLOS conditions, but also greatly improve the transmitter-receiver distance estimation. In addition, the proposed algorithms are robust to changes in environments and signal properties, and conditions without any LOS anchors. That is, algorithms can be trained on one environment and be utilized in another, which makes the algorithms, to some degree, generic to a variety of user locations and greatly improves the potential use of our algorithms in real world applications.

While designed for implementation on mobile devices, the limitation of the proposed algorithms is the costly training phase. To reduce or even eliminate the training phase requires some other information, either from the environments like the map and the location of access points or from the existing algorithm database like the training data in some other buildings. Therefore, our future work will incorporate such information to develop online learning algorithms or unsupervised machine

learning algorithms to identify the LOS/NLOS conditions. Alternatively, future models could also be initialized with our existing data sets and then adapted to new environments. In addition, the proposed techniques in this study have not accounted for some other interesting problems, e.g., the automatic switching between static and dynamic settings. These problems also present interesting directions for future work.

ACKNOWLEDGMENT

The authors would like to thank the anonymous reviewers for their comments and suggestions to improve the paper. They also acknowledge the support of the EPSRC through grants EP/L00416X/1.

REFERENCES

[1] H.-Q. Lai, A. S. Ibrahim, and K. J. R. Liu, "Wireless network cocast: Location-aware cooperative communications with linear network coding," *IEEE Trans. Wireless Commun.*, vol. 8, no. 7, pp. 3844–3854, Jul. 2009.

[2] S. Ilarri, E. Mena, and A. Illarramendi, "Location-dependent queries in mobile contexts: Distributed processing using mobile agents," *IEEE Trans. Mobile Comput.*, vol. 5, no. 8, pp. 1029–1043, Aug. 2006.

[3] P. Bahl and V. N. Padmanabhan, "RADAR: An in-building RF-based user location and tracking system," in *Proc. 19th Annu. IEEE INFOCOM*, Tel-Aviv, Israel, 2000, vol. 2, pp. 775–784.

[4] C. Figuera, I. Mora, and A. Guerrero, "Nonparametric model comparison and uncertainty evaluation for signal strength indoor location," *IEEE Trans. Mobile Comput.*, vol. 8, no. 9, pp. 1250–1264, Sep. 2009.

[5] Y. Gu, A. Lo, and I. Niemegeers, "A survey of indoor positioning systems for wireless personal networks," *IEEE Commun. Surveys Tuts.*, vol. 11, no. 1, pp. 13–32, 2009.

[6] L. Yang and G. B. Giannakis, "Ultra-wideband communications: An idea whose time has come," *IEEE Signal Process. Mag.*, vol. 21, no. 6, pp. 26–54, Nov. 2004.

[7] A. F. Molisch, "Ultra-wide-band propagation channels," *Proc. IEEE* , vol. 97, no. 2, pp. 353–371, Feb. 2009.

[8] M. Z. Win and R. A. Scholtz, "Characterization of ultra-wide bandwidth wireless indoor channels: A communication-theoretic view," *IEEE J. Sel. Areas Commun.*, vol. 20, no. 9, pp. 1613–1627, Dec. 2002.

[9] H. Kim and J. Choi, "Advanced indoor localization using ultrasonic sensor and digital compass," in *Proc. ICCAS*, Seoul, Korea, Oct. 2008, pp. 223–226, Ieee.

[10] B. Mobedi and G. Nejat, "3-D active sensing in time-critical urban search and rescue missions," *IEEE/ASME Trans. Mechatron.*, vol. 17, no. 6, pp. 1111–1119, Dec. 2012.

[11] G. Biffi Gentili, F. Dori, and E. Iadanza, "Dual-frequency active RFID solution for tracking patients in a children's hospital. Design method, test procedure, risk analysis, and technical solution," *Proc. IEEE*, vol. 98, no. 9, pp. 1656–1662, Sep. 2010.

[12] R. J. Vetter, U. Varsbney, and R. Kalakota, "Mobile commerce: A new frontier," *Computer*, vol. 33, no. 10, pp. 32–38, Oct. 2000.

[13] J. A. Dabin, A. M. Haimovich, and H. Grebel, "A statistical ultra-wideband indoor channel model and the effects of antenna directivity on path loss and multipath propagation," *IEEE J. Sel. Areas Commun.*, vol. 24, no. 4, pp. 752–758, Apr. 2006.

[14] K. Li, M. A. Ingram, and A. V. Nguyen, "Impact of clustering in statistical indoor propagation models on link capacity," *IEEE Trans. Commun.*, vol. 50, no. 4, pp. 521–523, Apr. 2002.

[15] C. Lim, J. L. Volakis, K. Sertel, R. W. Kindt, and A. Anastasopoulos, "Indoor propagation models based on rigorous methods for site-specific multipath environments," *IEEE Trans. Antennas Propag.*, vol. 54, no. 6, pp. 1718–1725, Jun. 2006.

[16] I. Guvenc, C. Chong, and F. Watanabe, "NLOS identification and mitigation for UWB localization systems," in *Proc. IEEE WCNC*, 2007, pp. 1571–1576.

[17] A. Maali, A. Ouldali, H. Mimoun, and G. Baudoin, "Joint TOA estimation and NLOS identification for UWB localization systems," in *Proc. 3rd Int. Conf. SENSORCOMM*, Athens, Greece, Jun. 2009, pp. 212–216.

[18] Y. Qi, H. Kobayashi, and H. Suda, "Analysis of wireless geolocation in a non-line-of-sight environment," *IEEE Trans. Wireless Commun.*, vol. 5, no. 3, pp. 3–5, Mar. 2006.

[19] S. Venkatesh and R. M. Buehrer, "Non-line-of-sight identification in ultra-wideband systems based on received signal statistics," *IET Microw. Antennas Propag.*, vol. 1, no. 6, pp. 1120–1130, Dec. 2007.

[20] Y. Jo, J. Lee, D. Ha, and S. Kang, "Accuracy enhancement for UWB indoor positioning using ray tracing," in *Proc. IEEE/ION Position. Loc. Navigat. Symp.*, 2006, pp. 565–568.

[21] J. Khodjaev, Y. Park, and A. Saeed Malik, "Survey of NLOS identification and error mitigation problems in UWB-based positioning algorithms for dense environments," *Ann. Telecommun.*, vol. 65, no. 5/6, pp. 301–311, Jun. 2010.

[22] S. Maran, W. M. Gifford, and H. Wymeersch, "NLOS identification and mitigation for localization based on UWB experimental data," *IEEE J. Sel. Areas Commun.*, vol. 28, no. 7, pp. 1026–1035, Sep. 2010.

[23] K. Yu, Y. J. Guo, and S. Member, "Statistical NLOS identification based on AOA, TOA, and signal strength," *IEEE Trans. Veh. Technol.*, vol. 58, no. 1, pp. 274–286, Jan. 2009.

[24] H. Wymeersch and S. Maranò, "A machine learning approach to ranging error mitigation for UWB localization," *IEEE Trans. Commun.*, vol. 60, no. 6, pp. 1719–1728, Jun. 2012.

[25] P. Chen, "A non-line-of-sight error mitigation algorithm in location estimation," in *Proc. IEEE WCNC*, 1999, pp. 316–320.

[26] X. Li, "An iterative NLOS mitigation algorithm for location estimation in sensor networks," in *Proc. 15th IST Mobile Wireless Commun. Summit*, Miconos, Greece, 2006, pp. 1–5.

[27] S. Nawaz and N. Trigoni, "Convex programming based robust localization in NLOS prone cluttered environments," in *Proc. 10th Int. Conf. IPSN*, Chicago, IL, USA, 2011, pp. 318–329.

[28] C. G. Koay and P. J. Basser, "Analytically exact correction scheme for signal extraction from noisy magnitude MR signals," *J. Magn. Reson.*, vol. 179, no. 2, pp. 317–322, Apr. 2006.

[29] C. Tepedelenlioglu, A. Abdi, and G. B. Giannakis, "The Ricean K factor: Estimation and performance analysis," *IEEE Trans. Wireless Commun.*, vol. 2, no. 4, pp. 799–810, Jul. 2003.

[30] R. Caruana and A. Niculescu-Mizil, "An empirical comparison of supervised learning algorithms," in *Proc. 23rd ICML*, Pittsburgh, PA, USA, 2006, pp. 161–168.

[31] M. Buhmann, *Radial Basis Functions: Theory and Implementations*, 1st ed. Cambridge, U.K.: Cambridge Univ. Press, 2003.

[32] J. Suykens and J. Vandewalle, "Least squares support vector machine classifiers," *Neur. Process. Lett.*, vol. 9, no. 3, pp. 293–300, Jun. 1999.

[33] H. W. Kuhn and A. W. Tucker, "Nonlinear programming," in *Proc. 2nd Berkeley Symp. Math. Statist. Probab.*, Berkeley, CA, USA, 1951, pp. 481–492.

[34] C. E. Rasmussen and C. K. I. Williams, *Gaussian Processes for Machine Learning*, 2nd ed., vol. 14. Cambridge, MA, USA: MIT Press, Apr. 2006.

[35] E. L. Snelson, "Flexible and efficient gaussian process models for machine learning," Ph.D. dissertation, Gatsby Comput. Neurosci. Unit, Univ. College London, London, U.K., 2007.

[36] C. E. Rasmussen and C. Williams, *Gaussian Process for Machine Learning*, 2nd ed. Cambridge, MA, USA: MIT Press, 2006.

[37] C. M. Bishop, *Neural Networks for Pattern Recognition*, vol. 92. London, U.K.: Oxford Univ. Press, Dec. 1997.

[38] C. Williams and D. Barber, "Bayesian classification with Gaussian processes," *IEEE Trans. Pattern Anal. Mach. Intell.*, vol. 20, no. 12, pp. 1342–1351, 1998.

[39] H. Nickisch and C. Rasmussen, "Approximations for binary Gaussian process classification," *J. Mach. Learn. Res.*, vol. 9, no. 2008, pp. 2035–2078, 2008.

[40] K. Cheung and R. D. Murch, "A new empirical model for indoor propagation prediction," *IEEE Trans. Veh. Technol.*, vol. 47, no. 3, pp. 996–1001, Aug. 1998.

[41] W. Honcharenko, H. L. Bertoni, and J. Dailing, "Mechanisms governing propagation between different floors in buildings," *IEEE Trans. Antennas Propag.*, vol. 41, no. 6, pp. 787–790, Jun. 1993.

[42] W. Honcharenko, H. Bertoni, J. Dailing, J. Qian, and H. Yee, "Mechanisms governing UHF propagation on single floors in modern office buildings," *IEEE Trans. Veh. Technol.*, vol. 41, no. 4, pp. 496–504, Nov. 1992.

[43] X. Zhou, Z. Zhang, G. Wang, and X. Yu, "Practical conflict graphs for dynamic spectrum distribution," in *Proc. ACM SIGMETRICS*, 2013, pp. 5–16.

[44] A. Dempster, N. Laird, and D. Rubin, "Maximum likelihood from incomplete data via the EM algorithm," *J. Roy. Statist. Soc.*, vol. 39, no. 1, pp. 1–38, 1977.

[45] M. Youssef and A. Agrawala, "The Horus WLAN location determination system," in *Proc. MobiSys*, 2005, pp. 205–218.

[46] N. K. Sharma, "A weighted center of mass based trilateration approach for locating wireless devices in indoor environment," in *Proc. Int. MobiWac*, New York, NY, USA, 2006, pp. 112–115.
[47] H. Shi, X. Li, Y. Shang, and D. Ma, "Cramer-Rao bound analysis of quantized RSSI based localization in wireless sensor networks," in *Proc. 11th ICPADS*, Fukuoka, Japan, 2005, vol. 2, pp. 32–36.

Zhuoling Xiao is currently pursuing the Ph.D. degree in computer science at University of Oxford. His research interests focus on sensor networks, including localization, communication and coordination protocols for networked sensor nodes, and machine learning techniques for sensor networks and localization.

Hongkai Wen received the Ph.D. degree in computer science from the University of Oxford. He is currently a Postdoctoral Researcher at the Department of Computer Science, University of Oxford. His research interests are in sensor networks, localization and navigation, and probabilistic machine learning.

Andrew Markham received the Bachelor's and Ph.D. degrees in electrical engineering from the University of Cape Town, South Africa, in 2004 and 2008, respectively. He is currently an Associate Professor in the Department of Computer Science, University of Oxford, working in the Sensor Networks Group. His research interests include low power sensing, embedded systems and magneto-inductive techniques for positioning and communication.

Niki Trigoni received the Ph.D. degree at the University of Cambridge in 2001. She became a Postdoctoral Researcher at Cornell University during 2002–2004 and a Lecturer at Birkbeck College during 2004–2007. Currently, she is an Associate Professor at the Department of Computer Science, University of Oxford. Since moving to Oxford in 2007, she established the Sensor Networks Group, and has conducted research in communication, localization and in-network processing algorithms for sensor networks. Her recent and ongoing projects span a wide variety of sensor networks applications, including indoor/underground localization, wildlife sensing, road traffic monitoring, autonomous (aerial and ground) vehicles, and sensor networks for industrial processes.

Phil Blunsom received the Ph.D. degree from the University of Melbourne, Australia, under the supervision of Timothy Baldwin, Steven Bird, and James Curran. He is currently an Associate Professor at the Department of Computer Science, University of Oxford. Previously, he was a Research Fellow in the School of Informatics, University of Edinburgh, and part of the Machine Translation research group, where he worked on the application of machine learning techniques to machine translation with Miles Osborne.

Jeff Frolik (S'85–M'95–SM'11) received the B.S.E.E. degree from the University of South Alabama in 1986, the M.S.E.E. degree from the University of Southern California in 1988 and the Ph.D. degree in electrical engineering systems from the University of Michigan in 1995. He is an Associate Professor in the School of Engineering, University of Vermont.